Journal of Materials Chemistry C

Accepted Manuscript

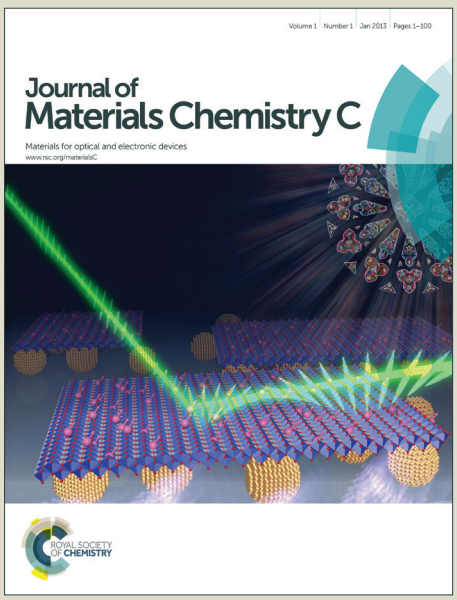

ROYAL SOCIETY OF CHEMISTRY

www.rsc.org/materialsC

Journal Name

ARTICLE

Conjugated polymers with deep LUMO levels for field-effect transistors and polymer-polymer solar cells

Received 00th January 20xx,
Accepted 00th January 20xx

DOI: 10.1039/x0xx00000x

www.rsc.org/

Andong Zhang,[a] Chengyi Xiao,[a] Dong Meng,[a] Qiang Wang,[b] Xiaotao Zhang,*[a] Wenping Hu,[a,c] Xiaowei Zhan,[d] Zhaohui Wang,*[a] René A. J. Janssen[b] and Weiwei Li*[a]

Three thiazole-bridged DPP polymers with deep lowest unoccupied molecular orbital (LUMO) levels were designed for field-effect transistors (FETs) and polymer-polymer solar cells. By introducing thiazole-thiazole coupled segments, perfluoroalkyl side chains or strong electron-deficient naphthalenediimide units into the conjugated backbone thethreethiazole-bridged DPP polymers haveLUMO levelsof -4.0 – -4.4 eV. The three DPP polymers exhibit optical absoption in the near-infrared, crystallinity and electron mobility around 0.01 $cm^2 V^{-1} s^{-1}$ in bottom contact FETs. The polymers were applied as electron acceptors in polymer-polymer solar cells to provide PCEsaround 0.4%. The low PCEs are mainly due to low short-circuit currents (J_{sc}) and attributed to large phase separation. Our results demonstrate several efficient strategies to lower the energy levels of conjugated polymers in order to be used as universal acceptors for photovoltaic cells.

Introduction

Bulk-heterojunction polymer solar cells comprising conjugated polymers as electron donor and fullerene derivatives as electron acceptor have successfully achieved power conversion efficiencies (PCEs) above 10% in recent years.[1-3] Application of conjugated polymers as electron acceptor to replace fullerene derivatives also attracts increasing attention,[4] even though polymer-polymer solar cells provide lower maximum PCEs of around 6% than polymer-fullerene solar cells.[5 - 8] Compared to the small-molecule fullerene derivatives, extended conjugated polymers provide better thermal stability of the morphology in photovoltaic devices. In addition, the chemical structure of polymer acceptors can be intentionally modified to tune their absorption spectra, energy levels, charge transport properties and crystallinity. It can be expected that the PCE of polymer-polymer solar cells will approach the PCE of polymer-fullerene solar cells when new polymer acceptors are systematically explored together with morphology and device optimization.

The success of fullerene derivatives such as [6,6]-phenyl-C_{71}-butyric acid methyl ester ([70]PCBM) in high efficient photovoltaic cells is mainly attributed to its high electron mobility, high crystallinity and suitable energy level for charge separation and transportation.[9] PCBM possesses a deep lowest unoccupied molecular orbital (LUMO) level below -4.0 eV and a highest occupied molecular orbital (HOMO) level below -6.0 eV)[10] and can be applied as almost universal electron acceptor in combination with numerous conjugated polymers as electron donor. Polymer acceptors with a LUMO below -4.0 eV have also been reported and are generally based on perylenediimide (PDI)[11 - 13] and naphthalenediimide (NDI) derivatives.[8, 14 - 16] Other building blocks, such as benzothiadiazole (BT),[17] isoindigo[18] and diketopyrrolopyrrole (DPP),[7, 19 - 22] have also been used in electron accepting polymers for polymer-polymer solar cells, but these usually possess higher-lying LUMO levels. While most studies focused on designing polymer acceptors with high-lying LUMO to afford a high open circuit voltage (V_{oc}) in polymer-polymer solar cells, it is also useful to explore polymer acceptors with lower lying LUMO levels similar to PCBM.

In this work, we attempt to develop conjugated polymers as electron acceptor based on electron-deficient DPP units, aiming at obtaining a deep LUMO level. Several DPP-based conjugated polymers exhibit high hole and electron mobilities around 10 $cm^2 V^{-1} s^{-1}$[23-25] and high PCEs above 8% as electron donor.[26-28] When introducing thiazole (Tz) into the conjugated backbone of DPP polymers, the LUMO of resulting PDPP2TzT polymer is reduced -4.0 eV due to the electronegative imine nitrogens (C=N-C) and an electron mobility of 0.13 $cm^2 V^{-1} s^{-1}$has been achioeved.[21] As a consequence, PDPP2TzT can be successfully applied as electron acceptor to yield PCE of 2.9% in polymer-polymer solar cells.[21] High-lying LUMO of thiazole-

[a] Beijing National Laboratory for Molecular Sciences, CAS Key Laboratory of Organic Solids, Institute of Chemistry, Chinese Academy of Sciences, Beijing 100190, P. R. China. E-mail: zhangxt@iccas.ac.cn or wangzhaohui@iccas.ac.cn or liweiwei@iccas.ac.cn
[b] Molecular Materials and Nanosystems, Eindhoven University of Technology P.O. Box 513, 5600 MB Eindhoven, The Netherlands
[c] Collaborative Innovation Center of Chemical Science and Engineering (Tianjin) & Department of Chemistry, School of Science, Tianjin University, Tianjin 300072, China.
[d] Department of Materials Science and Engineering, College of Engineering, Peking University, Beijing 100871, China.
† Electronic Supplementary Information (ESI) available. See
DOI: 10.1039/x0xx00000x

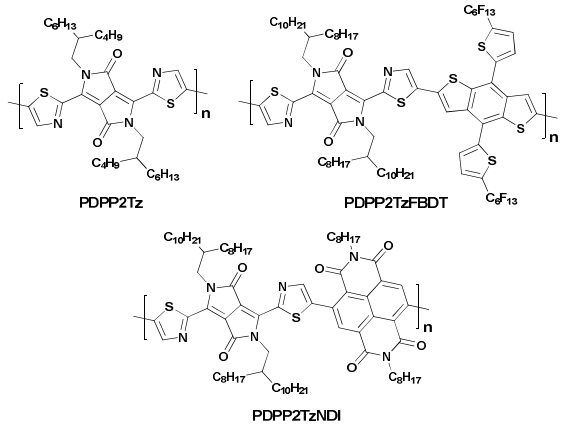

Fig. 1 Chemical structures of thiazole-bridged DPP polymers with deep LUMO levels.

bridged DPP polymers can be realized by introducing electron-rich copolymerized units into conjugated backbone.[22]

In order to achieve a low-lying LUMO in DPP polymers, three thiazole-bridged DPP polymers were designed and synthesized, as shown in Fig. 1. We show below that PDPP2Tz with thiazole-thiazole coupled segments has a LUMO of -4.03 eV. In PDPP2TzFBDT, where Tz-DPP-Tz alternates with perfluoroalkyl thiophene substituted benzodithiophene (FBDT) the LUMO is lowered to -4.16 eV. Further deepening of the LUMO to -4.4 eV is realized in PDPP2TzNDI, an acceptor-acceptor polymer consisting of Tz-DPP-Tz and NDI. These three polymers possess electron mobilities around 0.01 $cm^2 V^{-1} s^{-1}$ in bottom contact field-effect transistors (FETs). The polymers were applied in polymer solar cells as electron acceptor, but provided low PCEs of 0.4%. Our results pave the efficient way to design polymer acceptors with deep LUMO levels that can be used as universal electron acceptors for polymer-polymer solar cells.

Experimental

Materials and Measurements

All synthetic procedures were performed under Ar atmosphere. Commercial chemicals were used as received. THF and toluene were distilled from sodium under Ar atmosphere and benzophenone was used as indicator. 2-Perfluorohexylthiophene, [29] 3,6-bis(5-bromothiazol-2-yl)-2,5-bis(2-butyloctyl)pyrrolo[3,4-*c*]pyrrole-1,4(2*H*,5*H*)-dione (**4**), [30] 3,6-bis(5-bromothiazol-2-yl)-2,5-bis(2-octyldodecyl)pyrrolo[3,4-*c*]pyrrole-1,4(2*H*,5*H*)-dione (**6**),[22] 2,7-dioctyl-4,9-bis(trimethylstannyl)benzo[*lmn*][3,8]phenanthroline-1,3,6,8(2*H*,7*H*)-tetraone (**7**)[31] and the polymer PDPP5T[32] were synthesized according to literature procedures.

^{1}H-NMR and ^{13}C-NMR spectra were recorded at 400 MHz and 100 MHz on a Bruker AVANCE spectrometer with $CDCl_3$ as the solvent and tetramethylsilane (TMS) as the internal standard. Molecular weight of DPP polymers was determined with GPC at 140 ^{o}C on a PL-GPC 220 system using a PL-GEL 10μm MIXED-B column and *ortho*-dichlorobenzene (*o*-DCB) as the eluent against polystyrene standards. Low concentration of0.1 mg mL^{-1} polymer in *o*-DCB was applied to reduce aggregation. Electronic spectra were recorded on a JASCO V-570 spectrometer. Cyclic voltammetry was performed under an inert atmosphere with a scan rate of 0.1 V s^{-1} and 1M tetrabutylammonium hexafluorophosphate in acetonitrile as the electrolyte. An ITO glass slide cover with a thin layer polymer (approx. 20 nm) was used as working electrode. The counter and reference electrodes were Pt wire and Ag/AgCl, respectively. All potentials are referenced versus Fc/Fc^+. X-Ray diffraction (XRD) measurements were performed in reflection mode at 40 kV and 200 mA with Cu Kα radiation using a 2-kW Rigaku D/max-2500 X-ray diffractometer. Density functional theory (DFT) calculations were performed at the B3LYP/6-31G* level of theory by using the Gaussian 09 program package. Atomic force microscope (AFM) images were recorded by using a Digital Instruments Nanoscope IIIa Multimode atomic force microscope in tapping mode.

Organic field-effect transistors were fabricated using heavily doped silicon wafers as the common gate electrode with a 300 nm thermally oxidized SiO_2 layer which was modified by OTS as gate dielectric. Electrodes of Au (25 nm) were vacuum deposited first and then polymer thin films were spin coated on the substrate from chloroform solution with thickness around 30 – 50 nm. The devices were thermally annealed at temperatures of (140-160 °C) in a high vacuum chamber for 2 hours, cooled down and then moved into glovebox filled with N_2. The devices were measured on an Agilent B1500 semiconductor parameter analyser at room temperature.

Photovoltaic devices were made by spin coating poly-(ethylenedioxythiophene):poly(styrene sulfonate) (PEDOT:PSS) (Clevios P, VP AI 4083) onto precleaned, patterned indium tin oxide (ITO) substrates (15 Ω per square). The photoactive layer was deposited by spin coating a chloroform solution containing PDPP5T and DPP polymer acceptors with 1:1 (w/w) or 2:1 (w/w) ratio and the appropriate amount of processing additive such as diiodooctane (DIO), 1-chloronaphthalene (1-CN) or *o*-DCB. Ca (20 nm) and Al (100 nm) were deposited by vacuum evaporation at ~1×10^{-5} Pa as the back electrode. The active area of the cells was 0.04 cm^2. An XES-70S1 (SAN-EI electric Co., Ltd.) solar simulator (AAA grade, 70 ×70 mm^2 photobeam size) coupled with AM 1.5G solar spectrum filters was used as the light source, and the optical power at the sample was 100 mW cm^{-2}. A 2 ×2 cm^2 monocrystalline silicon reference cells (SRC-1000-TC-QZ) was purchased from VLSI standards Inc. The current-voltage (*I-V*) measurement of the devices was conducted using a computer-controlled Agilent B2912A Precision Source/Measure Unit. The extern quantum efficiency (EQE) spectrum was measured using a Solar Cell Spectral Response Measurement System QE-R3011 (Enlitech Co., Ltd.). The light intensity at each wavelength was calibrated using a standard single crystal Si photovoltaic cell.

4,8-bis(5-perfluorohexylthiophen-2-yl)benzo[1,2-*b*:4,5-*b'*]dithiophene (2)

n-Butyllithium (2.4 M in hexane, 2.50 mL, 6.0 mmol) was added dropwise to a solution of 2-perfluorohexylthiophene

(2.20 g, 5.5 mmol) in THF (15 mL) at -78 °C. The mixture was stirred for 2 h. Subsequently, 4,8-dehydrobenzo-[1,2-*b*:4,5-*b'*]dithiophene-4,8-dione (0.55 g, 2.5 mmol) (**1**) was added to the reaction mixture and stirred for 1 h at -78 °C. The mixture was then warmed to room temperature and stirred overnight. A mixture of $SnCl_2 \cdot 2H_2O$ (9 g, 40 mmol) in 10% HCl (16 mL) was added and the mixture was stirred for additional 1.5 h, after which it was poured into ice water. The mixture was extracted with petroleum ether twice and the combined organic phases were concentrated to obtain the crude compound **2**. Further purification was carried out by column chromatography on silica gel using petroleum ether as the eluent to obtain pure compound **2** as pale yellow viscous liquid (1.35 g, yield 55%).^{1}H NMR ($CDCl_3$): δ = 7.60 (d, 2H), 7.55 (s, 4H), 7.50 (d, 2H). ^{19}F NMR ($CDCl_3$): δ = −80.72, −101.09, −121.35, −122.69 , −126.01. MS (MALDI): calculated: 989.91, found: 989.9 (M^+).

(4,8-bis(5-perfluorohexylthiophen-2-yl)benzo[1,2-*b*:4,5-*b'*]dithiophene-2,6-diyl)bis(trimethylstannane) (3)

A solution of **2** (0.75 g, 0.76 mmol) in THF (15 mL) at -78 °C was placed in a 50 mL argon purged flask, and then n-butyllithium (1.6 M in hexane, 1 mL, 1.6 mmol) was added. The reaction mixture was then stirred for 2 h at -78 °C. Subsequently, trimethyltin chloride (1.0 M in hexane, 1.7 mL, 1.7 mmol) was added and the mixture was stirred overnight at ambient temperature. Then, the mixture was extracted by dichloromethane and the combined organic phase was concentrated. Further purification was carried out by recrystallization using ethanol to obtain the pure compound as a yellow solid (0.45 g, yield 45%). ^{1}H NMR ($CDCl_3$): δ = 7.61 (d, 2H), 7.56 (s, 2H), 7.52 (d, 2H), 0.42 (s, 18H). ^{13}C NMR (101 MHz, $CDCl_3$): δ = 145.41, 144.39, 143.67, 140.02, 137.54, 130.69, 130.13, 129.77, 129.48, 128.23, 120.96, 77.34, 77.23, 77.02, 76.71, -0.00, -6.46, -6.54, -8.32, -10.09, -10.18. ^{19}F NMR ($CDCl_3$): δ = −80.73, −100.92, −121.42, −122.65 , −126.00.

PDPP2Tz

To a degassed solution of monomer (**4**) (66.93 mg, 0.084 mmol), hexabutylditin (48.73 mg, 0.084 mmol) (**5**) in toluene (1.5 mL) and DMF (0.15 mL), $Pd_2(dba)_3$ (2.29 mg, 2.5 µmol), triphenylphosphine (PPh_3) (2.62 mg, 10.0 µmol) and CuI (3.24 mg, 0.017 mmol)were added. The mixture was stirred at 115 °C for 24 h, after which it was precipitated into methanol and filtered through a Soxhlet thimble. The polymer was extracted with acetone, hexane and chloroform. The chloroform fraction was reduced and the polymer was precipitated in acetone. The polymer was collected by filtering over a 0.45 µm PTFE membrane filter and dried in a vacuum oven to yield PDPP2Tz (36 mg, 67%) as a dark solid. GPC (*o*-DCB, 140 °C): M_n = 8.6 kg mol^{-1} and PDI = 1.72.

PDPP2TzFBDT

To a degassed solution of the monomer **6** (75.83 mg, 0.074 mmol), **3** (97.40 mg, 0.074 mmol) in toluene (1.5 mL) and DMF (0.15 mL), $Pd_2(dba)_3$ (2.01 mg, 2.2 µmol) and triphenylphosphine (PPh_3) (2.31 mg, 8.8 µmol) were added. The mixture was stirred at 115 °C for 24 h, after which it was precipitated in methanol and filtered through a Soxhlet thimble. The polymer was extracted with acetone, hexane and chloroform. The chloroform fraction was reduced and the polymer was precipitated in acetone. The polymer was collected by filtering over a 0.45 µm PTFE membrane filter and dried in a vacuum oven to yield PDPP2TzFBDT (106 mg, 77%) as a dark solid. GPC (*o*-DCB, 140 °C): M_n = 13.1 kg mol^{-1} and PDI = 1.74 (The polymer is only partially dissolved in *o*-DCB at 140 °C).

PDPP2TzNDI

Same procedure as for PDPP2Tz was used, but now **6** (81.70 mg, 0.080 mmol) and **7** (85.58 mg, 0.080 mmol) were used as the monomers. Yield: 72 mg, 67%. GPC (*o*-DCB, 140 °C): M_n = 44.9 kg mol^{-1} and PDI = 2.53.

Results and discussion

Synthesis

The synthetic routes for the monomers and polymers are presented in Scheme 1. The bistannyl-FBDT (**3**) monomer was synthesized similar to the literature[33] and can be recrystallized to high purity, which is beneficial for efficient polymerization. The polymers were prepared from the dibromo-2TzDPP monomers (**4** or **6**) and bisstannyl compounds (**3**, **5**, **7**) by Stille polymerization, in which $Pd_2(dba)_3/PPh_3$ with or without CuI as

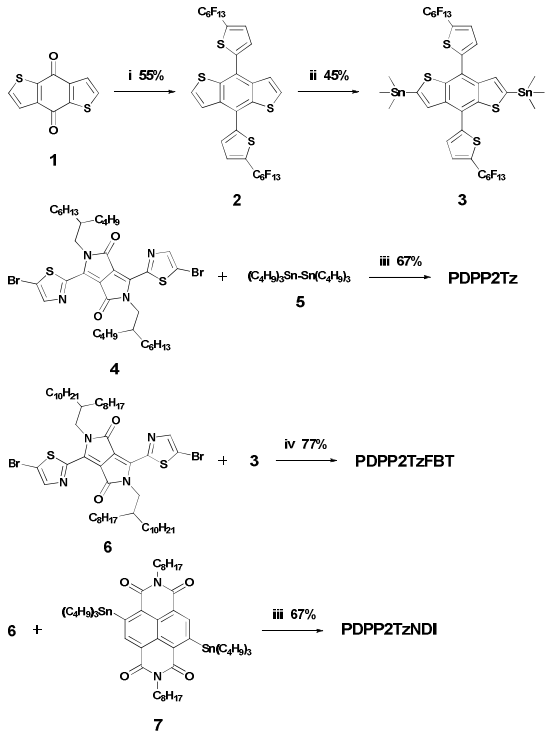

Scheme 1 synthesis route of thiazole-bridged DPP polymers. (i) 2-perfluorohexylthiophene, THF, n-BuLi, -78 °C; benzo[1,2-b:4,5-b']dithiophene-4,8-dione, room temperature; then $SnCl_2 \cdot 2H_2O$, HCl, rt. (ii) n-BuLi, THF, -78 °C, $Sn(CH_3)_3Cl$, room temperature. (iii) $Pd_2(dba)_3/PPh_3$/CuI in toluene/DMF (10:1, v/v) at 115 °C. (iv) $Pd_2(dba)_3/PPh_3$ in toluene/DMF (10:1, v/v) at 115 °C.

Table 1 Molecular Weight, Optical and electrochemical Properties of the DPP Polymers.

				$CHCl_3$ solution			Film				
Polymer	M_n[a] (kg mol^{-1})	M_w[a] (kg mol^{-1})	PDI	λ_{peak} (nm)	λ_{onset} (nm)	E_g^{sol} (eV)	λ_{peak} (nm)	λ_{onset} (nm)	E_g^{film} (eV)	*LUMO* (eV)[c]	*HOMO* (eV)[d]
PDPP2Tz	8.6	14.9	1.72	716, 786	832	1.49	720, 781	904	1.37	-4.03	-5.40
PDPP2TzFBDT	13.1[b]	22.7[b]	1.74	670, 712	776	1.60	673, 719	787	1.58	-4.16	-5.74
PDPP2TzNDI	44.9	113.5	2.53	645	779	1.59	669	808	1.53	-4.40	-5.93

[a]Determined with GPC at 140 °C using *o*-DCB as the eluent. [b]Determined by low molecular weight fraction dissolved in *o*-DCB at 140 °C. [c]Determined using a work function value of -5.23 eV for Fc/Fc$^+$. [d]Determined as E_{LUMO}–E_g^{film}.

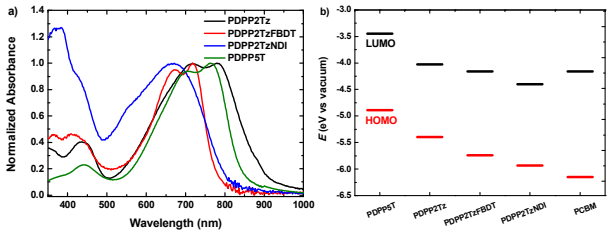

Fig. 2 (a) Optical absorption spectra of the polymers in solid state films and (b) HOMO and LUMO levels determined from cyclic voltammetry.

catalyst and toluene/DMF as solvent were used to achieve optimized molecular weight. 2-Butyloctyl (BO) for PDPP2Tz and 2-octyldodecyl (OD) for PDPP2TzFBDT and PDPP2TzNDI were used as side chains on DPP to optimize solubility. The molecular weight of the polymers was determined by GPC measurement using *o*-DCB at 140 °C as eluent and a low polymer concentration of 0.1 mg/ml was used to reduce aggregation (Fig. S1, ESI†). PDPP2Tz has a relatively low molecular weight of M_n = 8.6 kg mol^{-1} (Table 1), which may be caused by the lower reactivity of hexabutylditin. Under the same polymerization conditions, PDPP2TzNDI gave a high M_n = 44.9 kg mol^{-1}. For PDPP2TzFBDT with perfluorohexyl side chains, the high molecular weight fraction was insoluble in *o*-DCB even at 140 °C, and only a low molecular weight fraction was measured, giving M_n = 13.1 kg mol^{-1}.

Optical and electrochemical properties

UV-vis absorption spectra of the DPP polymers in chloroform solution and as thin films are shown in Fig. S2 (ESI†) and Fig. 2a, and the data are summarized in Table 1. All polymers exhibit red-shifted absorption spectra in thin films compared to solution spectra, indicating aggregation in the solid state. PDPP2Tz has an optical band gap of E_g = 1.37 eV, which is lower than that of PDPP2TzT which has an additional thiophene as co-unit (E_g = 1.47 eV).[21] PDPP2TzFBDT has E_g = 1.58 eV, which is slightly higher than that of PDPP2TzBDT with benzodithiophene (BDT) (E_g = 1.53 eV).[22] PDPP2TzNDI with an electron-deficient DPP core and NDI give an E_g of 1.53 eV, which is much larger than its analogue PNDI-DPP (E_g = 1.15 eV) with thiophene as bridges,[34] indicating the strong influence of thiazole on the optical properties.

The frontier orbital energy levels of the polymers were determined by cyclic voltammetry (CV) on thin films (Fig. 2b, Table 1 and Fig. S3, ESI†). For comparison, [70]PCBM gave aLUMO of -4.16 eV and a HOMO of -6.15 eV in our measurement (Fig. S3b, ESI†). PDPP2Tz has a LUMO of -4.03 eV and HOMO of -5.40 eV. When introducing perfluorohexyl units, PDPP2TzFBDT shows a similar LUMO as [70]PCBM of -4.16 eV and a HOMO of -5.74 eV. It is interesting to note that PDPP2TzBDT, without perfluoroalkyl side groups, has a LUMO of -4.0 eV,[22] indicating that the side chains can effectively tailor the energy levels. Further lowering of LUMO and HOMO was realized by incorporating two electron-deficient units: DPP and NDI. PDPP2TzNDI has a LUMO of -4.40 eV and a HOMO at -5.93 eV. The deep LUMO of PDPP2TzNDI compared to that of PCBM should provide a larger driving force for exciton dissociation into free charges in polymer-polymer solar cells, but of course a concomitant loss in V_{oc}.

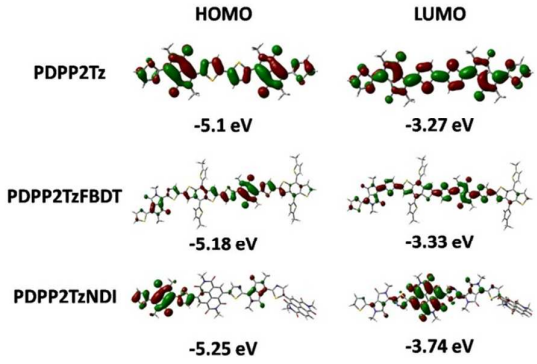

Fig. 3 DFT frontier molecular orbitals for the segments of PDPP2Tz, PDPP2TzFBDT and PDPP2TzNDI.

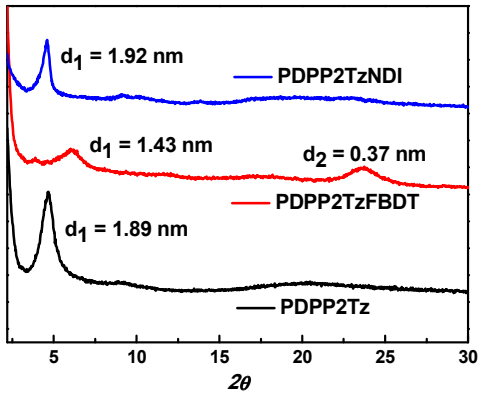

Fig. 4 X-ray diffraction patterns of thermally annealed DPP polymers thin films. Annealing temperature for PDPP2Tz, PDPP2TzFBDT and PDPP2TzNDI is 150 °C, 140 °C and 160 °C for 10 min.

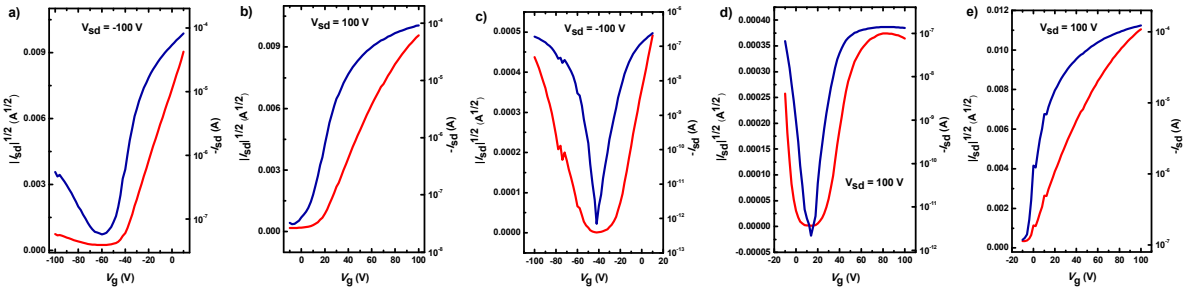

Fig. 5 Transfer characteristics for bottom-contact OFETs for the DPP polymers. (a) and (b) PDPP2Tz, (c) and (d) PDPP2TzFBDT and (e) PDPP2TzNDI. (a) and (c) for p-type, (b), (d) and (e) for n-type.

Table 2 Field-effect hole and electron mobility of the DPP polymers thin films after thermal annealing (TA) at high vacuum for 2 hours.

Polymer	TA (^oC)[a]	μ_h ($cm^2\ V^{-1}\ s^{-1}$)	μ_e ($cm^2\ V^{-1}\ s^{-1}$)
PDPP2Tz	150	7.3×10^{-4}	3×10^{-2}
PDPP2TzFBDT	140	4×10^{-4}	1.4×10^{-3}
PDPP2TzNDI	160	-	1.7×10^{-2}

[a]Temperature of thermal annealing

The delocalization of the frontier orbitals over the conjugated backbone and the expected energy levels were further studied by density functional theory (DFT) calculations on B3LYP/6-31G level (Fig. 3). In the DFT calculations methyl and trifluoromethyl units were used to replace of long alkyl chains and perfluorohexyl units in order to reduce the calculation time. For PDPP2Tz and PDPP2TzFBDT, both HOMO and LUMO levels are delocalized along the conjugated backbone. However, PDPP2TzNDI has more localized HOMO on the DPP-segment and LUMO on the NDI-segment. In addition, the calculated HOMO and LUMO levels show similar trends as in electro-chemical measurement that increase from PDPP2Tz to PDPP2TzFBDT and PDPP2TzNDI.

Thin polymer films on Si substrates were analysed by X-ray diffraction (XRD) to determine the molecular packing. The polymer thin films were drop cast from chloroform solutions and thermal annealed at the temperatures indicated in Table 2. The polymers exhibit (100) diffraction peaks at 2θ = 4.67° (PDPP2Tz), 6.17° (PDPP2TzFBDT) and 4.61° (PDPP2TzNDI), corresponding to lamellar spacings of 1.89 nm, 1.43 nm and 1.92 nm (Fig. 4). The PDPP2TzFBDT film also shows an additional broad peak (010) at 23.7°, corresponding to the π-π stacking distance of 0.37 nm.

Charge carrier mobility

The electron mobility of the conjugated polymers is important for the efficient polymer-polymer solar cells. High electron mobility assists charge transport to the electrodes and reduces recombination. The mobilities of the polymers were determined in a bottom gate – bottom contact FET configuration, where a highly n-doped Si wafer with a SiO_2 layer, which contained strip gold electrodes, was passivated with octadecyltrichlorosilane (OTS) self-assembled monolayers. DPP polymers were dissolved in chloroform and spin-coated on the substrates. The devices were thermally annealed at 140-160 °C (Table 2) and measured under inert atmosphere. Typical transistor transfer and output characteristics are shown in Fig. 5 and Fig. S4 (ESI†).OFETs based on the as cast polymer thin films were also characterized and showed much lower charge carrier mobilities (Table S1) than those of the devices with thermal annealing (Table 2). The improved mobilities after thermal annealing can be attributed to the enhanced crystallinity, which was also observed in other conjugated polymer FETs.[35] AFM revealed that the roughness of the polymer thin films was increased after thermal annealing, indicating better aggregation (Fig. S5, SI). PDPP2Tz and PDPP2TzFBDT exhibit ambipolar transfer characteristics with high electron mobility compared to their hole mobility (Fig. 5 and Table 2). PDPP2TzNDI only shows electron mobility of $1.7\times10^{-2}cm^2\ V^{-1}\ s^{-1}$. The electron mobilities of these DPP polymers are comparable to other electron acceptors such as P(NDI2OD-T2) in the same device configuration.[36]

Polymer-polymer solar cells performance

The DPP polymers in this work show optical absorption in the near-infrared, deep LUMO, crystallinity and sufficiently high electron mobility, making them of interest for application as electron acceptor for polymer-polymer solar cells. In this work, we selected another DPP polymer PDPP5T as electron donor to construct photovoltaic devices.[21] PDPP5T with DPP as core alternating with five thiophene rings as repeating units has been successfully applied into polymer-polymer solar cells combined with PDPP2TzT as electron acceptor.[21] By applying cyclic voltammetry as performed for the three acceptor DPP polymers, the HOMO and LUMO levels of PDPP5T were determined to be -4.89 eV and -3.45 eV (Fig. 2b and Fig. S3a, ESI†). Therefore, both the HOMO and LUMO offsets between PDPP5T and the DPP polymers in this work are larger than 0.3 eV, which ensures enough driving force for exciton dissociation into free charges.[37]

Polymer-polymer solar cells were fabricated by using ITO/PEDOT:PSS and Ca/Al as electrodes. The photo-active layers, consisting of PDPP5T blended with the thiazole-bridged DPP polymers were processed from chloroform solution, in which the processing additive, the ratio of donor to acceptor and the thickness of the active layer were optimized. Different high boiling point additives, such as DIO, 1-CN and *o*-DCB were examined, but 1-CN provided the best performance for all cells (Table S2). The *J-V* characteristicsare shown in Fig. 6a and the

Table 3 Solar cell parameters of optimized solar cells of PDPP5T:DPP polymers.

Polymer		J_{sc} (mA cm^{-2})	V_{oc} (V)	FF	PCE (%)
PDPP2Tz[a]	Normal	1.6	0.57	0.40	0.37
PDPP2TzFBDT[a]	Normal	0.77	0.61	0.39	0.19
PDPP2TzNDI[b]	Normal	2.2	0.53	0.36	0.42

[a]Ratio of donor to acceptor is 1:1. [b]Ratio of donor to acceptor is 2:1. Optimized spin coating solvent for active layer is $CHCl_3$ with 3% 1-CN as additive and the thickness of photo-active layer is around 90 nm.

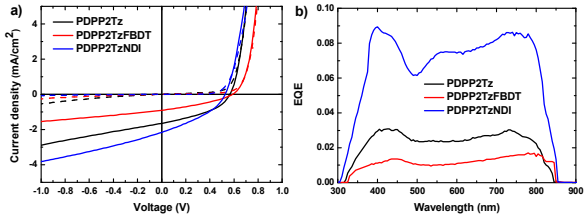

Fig. 6 (a) *J-V* characteristics in dark (dashed lines) and under white light illumination (solid lines) of optimized solar cells of PDPP5T blended with PDPP2Tz (1:1), PDPP2TzFBDT (1:1) or PDPP2TzNDI (2:1). (b) EQE of the same devices.

photovoltaic parameters are summarized at Table 3. All cells provide a moderate V_{oc} of 0.53– 0.61V, where PDPP2TzNDI with the deepest LUMO gave V_{oc} of 0.53 V. In comparison, PDPP5T:PCBM cells have been reported to give a V_{oc} of 0.57 V.[21] Therefore, the V_{oc} in these polymer–polymer solar cells confirm the similar or even lower LUMO levels compared to that of PCBM. However, all these cells show a low short circuit current density (J_{sc}) of 0.77 – 2.2 mA cm^{-2} and poor fill factor (FF) < 0.4. The low J_{sc} is reflected in a low external quantum efficiency (EQE) (Fig. 6b).The three cells display EQEs below 0.1 in their absorption region. As result, the PCE based on these cells ranged from 0.19% - 0.42%.

The low PCE in these cells needs to be discussed. Several parameters can influence the device performance, including photon absorption, exciton diffusion, charge separation, and charge transport into electrodes. Since in these donor-acceptor polymer-polymer systems, the HOMO-HOMO and LUMO-LUMO energy differences are higher than 0.3 eV efficient charge generation via exciton dissociation is expected. Therefore, we presume that exciton diffusion or charge transport and recombination limit the efficiency. When studying the morphology of the blend films by AFM (Fig. 7), large domains were found in all three systems, indicating that photo-generated excitons are prone to intrinsic recombination before they can diffuse to the interface between the donor and acceptor, where charges can be formed. Especially, for PDPP5T:PDPP2TzFBDT with perfluoroalkyl side chains, fibril-like structures were found that can be attributed to the demixed thin films between PDPP5T and PDPP2TzFBDT. It has been also reported that conjugated polymers bearing perfluoroalkyl chains had the tendency to self-aggregate into fibril-structures via fluorophobic effect.[38] Therefore, further improvement of PCE based on these polymer acceptors requires selecting suitable donor polymers and device optimization to achieve better phase separation.

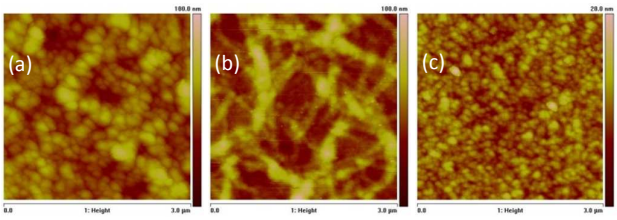

Fig. 7 AFM height image of optimized PDPP5T:DPP-polymers active layers spin coated from chloroform containing 3% vol. 1-CN. (a) PDPP2Tz, (b) PDPP2TzFBDT and (c) PDPP2TzNDI. Root mean square (RMS) roughness is 9.24 nm, 12.1 nm and 1.61 nm.

Conclusions

In this work, three thiazole-bridged DPP polymers with deep LUMO levels were designed and synthesized via Stille polymerization for application in FETs and polymer solar cells as electron acceptor. By applying thiazole-thiazole coupled segments, perfluoroalkyl side chains or strong electron-deficient moiety in the main chain as design strategy, the LUMO levels of DPP polymers could be adjusted to below -4.0 eV. The polymers also show near-infrared absorption and are semi-crystalline. The polymers were applied in bottom-contact FETs where they show an electron mobility around 0.01 cm^2 V^{-1} s^{-1}. The polymers were tested as electron acceptor for polymer-polymer solar cells in combination with another DPP polymer as donor to give a PCE of 0.4%. The low PCE was found to mainly originate from the large phase separation between the donor and acceptor, leading to a reduced J_{sc}. From this point, much effort is still needed to further improve the PCE based on these DPP polymers acceptors, such as the selection of donor materials and optimization of solution process technique.

Acknowledgements

We thanks Ralf Bovee at Eindhoven University of Technology (TU/e, Netherlands) for GPC analysis. This work was supported by the Recruitment Program of Global Youth Experts of China. The work was further supported by the Ministry of Science and Technology of China (2014CB643600, 2013CB933500), and the Strategic Priority Research Program (Grant No. XDB12030300) of the Chinese Academy of Sciences.

Notes and references

1 L. Dou, J. You, Z. Hong, Z. Xu, G. Li, R. A. Street and Y. Yang, *Adv. Mater.*, 2013, **25**, 6642-6671.
2 S. Zhang, L. Ye, W. Zhao, B. Yang, Q. Wang and J. Hou, *Sci. China Chem.*, 2015, **58**, 248-256.
3 Y. Liu, J. Zhao, Z. Li, C. Mu, W. Ma, H. Hu, K. Jiang, H. Lin,H. Ade and H. Yan, *Nat. Commun.*, 2014, **5**, 5293/1-8.
4 A. Facchetti, Mater. Today, 2013, **16**, 123–132.
5 Y. Zhou, T. Kurosawa, W. Ma, Y. Guo, L. Fang, K.Vandewal,Y. Diao, C. Wang, Q. Yan, J. Reinspach, J. Mei, A. L. Appleton, G. I. Koleilat, Y. Gao, S. C. B. Mannsfeld, A. Salleo, H. Ade, D. Zhao and Z. Bao, Adv. Mater., 2014, **26**, 3767–3772.
6 J. W. Jung, J. W. Jo, C.-C. Chueh, F. Liu, W. H. Jo, T. P. Russell and A. K. Y. Jen, *Adv. Mater.*, 2015, **27**, 3310-3317.

7 Y.-J. Hwang, T. Earmme, B. A. E. Courtright, F. N. Eberle and S. A. Jenekhe, *J. Am. Chem. Soc.*, 2015, **137**, 4424-4434.
8 D. Mori, H. Benten, I. Okada, H. Ohkita and S. Ito, *Energy Environ. Sci.*, 2014, **7**, 2939-2943.
9 T. B. Singh , N. Marjanovic , P. Stadler , M. Auinger , G. J. Matt, S. Günes , N. S. Sariciftci, R. Schwödiauer and S. Bauer, *J. Appl. Phys*., 2005, **97**, 083714.
10 S. Hellström, F. Zhang, O. Inganäs and M. R. Andersson, *Dalton T*, 2009, 10032-10039.
11 X. Zhan, Z. a. Tan, B. Domercq, Z. An, X. Zhang, S. Barlow, Y. Li, D. Zhu, B. Kippelen and S. R. Marder, *J. Am. Chem. Soc.*, 2007, **129**, 7246-7247.
12 Y. Zhou, Q. Yan, Y.-Q. Zheng, J.-Y. Wang, D. Zhao and J. Pei, *J. Mater. Chem. A*, 2013, **1**, 6609-6613.
13 Y. Zhou, T. Kurosawa, W. Ma, Y. Guo, L. Fang, K. Vandewal, Y. Diao, C. Wang, Q. Yan, J. Reinspach, J. Mei, A. L. Appleton, G. I. Koleilat, Y. Gao, S. C. B. Mannsfeld, A. Salleo, H. Ade, D. Zhao and Z. Bao, *Adv. Mater.*, 2014, **26**, 3767-3772.
14 X. Guo, A. Facchetti and T. J. Marks, *Chem. Rev.*, 2014, **114**, 8943-9021.
15 D. Mori, H. Benten, I. Okada, H. Ohkita and S. Ito, *Adv. Energy Mater.*, 2014, **4**, 1301001-1301006.
16 T. Earmme, Y.-J. Hwang, N. M. Murari, S. Subramaniyan and S. A. Jenekhe, *J. Am. Chem. Soc.*, 2013, **135**, 14960-14963.
17 D. Mori, H. Benten, J. Kosaka, H. Ohkita, S. Ito and K. Miyake, *ACS Appl. Mater. Interfaces*, 2011, **3**, 2924-2927.
18 R. Stalder, J. Mei, J. Subbiah, C. Grand, L. A. Estrada, F. So and J. R. Reynolds, *Macromolecules*, 2011, **44**, 6303-6310.
19 M.-F. Falzon, A. P. Zoombelt, M. M. Wienk and R. A. J. Janssen, *Phys Chem Chem Phys*, 2011, **13**, 8931-8939.
20 W. Li, T. Lee, S. J. Oh and C. R. Kagan, *ACS Appl. Mater. Interfaces*, 2011, **3**, 3874-3883.
21 W. Li, W. S. C. Roelofs, M. Turbiez, M. M. Wienk and R. A. J. Janssen, *Adv. Mater.*, 2014, **26**, 3304-3309.
22 W. Li, Y. An, M. M. Wienk and R. A. J. Janssen, *J. Mater. Chem. A*, 2015, **3**, 6756-6760.
23 J. Y. Back, H. Yu, I. Song, I. Kang, H. Ahn, T. J. Shin, S.-K. Kwon, J. H. Oh and Y.-H. Kim, *Chem. Mater.*, 2015, **27**, 1732-1739.
24 J. H. Park, E. H. Jung, J. W. Jung and W. H. Jo, *Adv. Mater.*, 2013, **25**, 2583-2588.
25 B. Sun, W. Hong, Z. Yan, H. Aziz and Y. Li, *Adv. Mater.*, 2014, **26**, 2636-2642.
26 H. Choi, S.-J. Ko, T. Kim, P.-O. Morin, B. Walker, B. H. Lee, M. Leclerc, J. Y. Kim and A. J. Heeger, *Adv. Mater.*, 2015, **27**, 3318-3324.
27 K. H. Hendriks, G. H. L. Heintges, V. S. Gevaerts, M. M. Wienk and R. A. J. Janssen, *Angew. Chem., Int. Ed.*, 2013, **52**, 8341-8344.
28 R. S. Ashraf, I. Meager, M. Nikolka, M. Kirkus, M. Planells, B. C. Schroeder, S. Holliday, M. Hurhangee, C. B. Nielsen, H. Sirringhaus and I. McCulloch, *J. Am. Chem. Soc.*, 2014, **137**, 1314-1321.
29 Z. Mao, K. Vakhshouri, C. Jaye, D. A. Fischer, R. Fernando, D. M. DeLongchamp, E. D. Gomez and G. Sauvé, *Macromolecules*, 2013, **46**, 103-112.
30 W. Li, K. H. Hendriks, A. Furlan, M. M. Wienk and R. A. J. Janssen, *J. Am. Chem. Soc.*, 2015, **137**, 2231-2234.
31 X. Zhang, C. Xiao, A. Zhang, F. Yang, H. Dong, Z. Wang, X. Zhan, W. Li and W. Hu, *To be submitted*.
32 W. Li, W. S. C. Roelofs, M. M. Wienk and R. A. J. Janssen, *J. Am. Chem. Soc.*, 2012, **134**, 13787-13795.
33 L. J. Huo, S. Q. Zhang, X. Guo, F. Xu, Y. F. Li and J. H. Hou, *Angew. Chem. Int. Ed.*, 2011, **50**, 9697-9702.
34 P. Wang, H. Li, C. Gu, H. Dong, Z. Xu and H. Fu, *Rsc Adv*, 2015, **5**, 19520-19527.
35 C. Li, N. Zheng, H. Chen, J. Huang, Z. Mao, L. Zheng, C. Weng, S. Tan and G. Yu, *Polym. Chem.*, 2015, DOI: 10.1039/C5PY00605H.
36 Z. Chen, Y. Zheng, H. Yan and A. Facchetti, *J. Am. Chem. Soc.*, 2009, **131**, 8-9.
37 C. J. Brabec, C. Winder, N. S. Sariciftci, J. C. Hummelen,A. Dhanabalan, P. A. van Hal, R. A. J. Janssen, *Adv. Funct. Mater.*, 2002, **12**, 709–712.
38 H. Jeong, B. Lim, D. Khim, M. Han, J. Lee, J. Kim, J. Yun, K. Cho, J. Park and D. Kim, *Adv. Funct. Mater.*, 2013, **25**, 6416-6422.

Graphic:

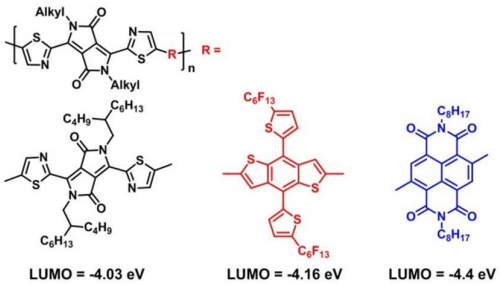

Text:

Three new diketopyrrolopyrrole-based conjugated polymers were developed with low-lying LUMO up to -4.4 eV for n-type field-effect transistors and polymer-polymer solar cells.